Journal of Sound and Vibration (1998) **214**(5), 793–803
Article No. sv981549

STABILITY AND BIFURCATION OF ROTOR MOTION IN A MAGNETIC BEARING

M. Chinta* and A. B. Palazzolo

Department of Mechanical Engineering, Texas A & M University, College Station, TX 77843-3367, *U.S.A.*

(*Received* 28 *February* 1997, *and in final form* 30 *January* 1998)

The equations of motion of a two-degrees-of-freedom mass in a magnetic bearing are non-linear in displacement, with geometric coupling of the magnetic bearing coupling the horizontal and vertical components of rotor motion. The non-linear forced response is studied in two ways: (1) using imbalance force; (2) using non-imbalance harmonic force. In the forced response, only periodic motion is investigated here. Stable periodic motion is obtained by numerical integration and by the approximate method of trigonometric collocation. Where unstable motion coexists with stable motion after a bifurcation of periodic motion, the unstable motion is obtained by the collocation method. The periodic motions' local stability and bifurcation behavior are obtained by Floquet theory. The parameters i.e., rotor speed, imbalance eccentricity, forcing amplitude, rotor weight, and geometric coupling are investigated to find regimes of non-linear behavior such as jumps and subharmonic motion.

1. INTRODUCTION

Non-linear rotor motion in rotating machinery is commonly caused by the non-linear characteristics of supporting bearings[1]. The bearings could be either conventional mechanical bearings (ball, journal, or fluid-film bearings, etc.) or active magnetic bearings which are electro-mechanical in nature. Various non-linear studies have been done on magnetic bearings. Several resonant frequencies are obtained for a one-degeee-of-freedom mass in a magnetic bearing where control current is only proportional to displacement, i.e., the bearing has non-linear stiffness [2]. An unstable limit cycle resulting from subcritical Hopf bifurcation of the rotor equilibrium position is caused by rotor gyroscopic effects [3]. It is, however, stabilized by a non-linear feedback control. Eddy currents result in lift and drag forces and cause coupling of rotor motion in the co-ordinate directions. These are predominant in a non-laminated radial bearing, where they cause the Hopf bifurcation of equilibrium position [4]. Multiple solutions are obtained at resonance, and fractal boundaries separate stable and unstable regions due to geometric coupling [5]. Stable quasiperiodic motion is obtained for large geometric coupling values if the rotor weight is neglected [6].

In solving non-linear differential equations, numerical integration is commonly used as no closed form solutions exist for strongly non-linear systems. Numerical integration may be inefficient for lightly damped systems. Moreover, the commonly used numerical integration schemes such as Runge–Kutta may not give all unstable solutions. However,

* Mechanical Engineering Technology Program.

0022–460X/98/300793 + 11 $30.00/0

a numerical method such as the continuation method may be used to obtain unstable solutions. The perturbation methods are useful for weakly non-linear systems, and the approximate (semi-analytical) methods are useful for strongly non-linear systems. The approximate methods that were used for rotor–bearing systems are the trigonometric collocation method, harmonic balance methods, the shooting method [7], and the finite difference method [8]. Here, the collocation method is chosen as it is easy to use, works well with any intitial guesses, and gives both stable and unstable periodic solutions. Since only periodic behavior is of interest here, the non-periodic responses are not investigated using the collocation method.

The trigonometric collocation method is a frequency domain method. It was used to obtain the non-linear frequency response curve of a flexible rotor in squeeze film dampers [9]. For a similar system, the collocation method was used with Floquet stability theory [10]. The collocation method was used to find the self-excited oscillations of a Van der Pol oscillator [11].

2. ROTOR-BEARING MODEL

An active magnetic bearing system includes a stator, sensors, and a feedback control system as shown in Figure 1. The stator has four pole-pairs. The commonly used control strategy is to have independent axis control, i.e., two opposing pole-pairs on the x-axis control the rotor motion in x-direction, and the other two pole-pairs are for y-axis motion control. The feedback control system generates a current that is proportional to the measured rotor displacement and velocity, i.e., a PD control is used. The controllers' PD gains for all four pole-pairs are taken to be the same. The rotor is one mass with two degrees of freedom. For a magnetic bearing, when the rotor position is offset from the axes of symmetry of the pole-pairs, the pole-pairs in the horizontal direction exert forces in both the horizontal and vertical directions. This geometric coupling of forces was discussed in reference [6].

The dimensionless equations of motion governing the unbalance response of a rotor are [6]

$$x'' = f_r - f_l + \alpha x(f_t + f_b) + E\Omega^2 \cos \Omega\tau, \tag{1}$$

$$y'' = f_t - f_b + \alpha y(f_r + f_l) + E\Omega^2 \sin \Omega\tau - G, \tag{2}$$

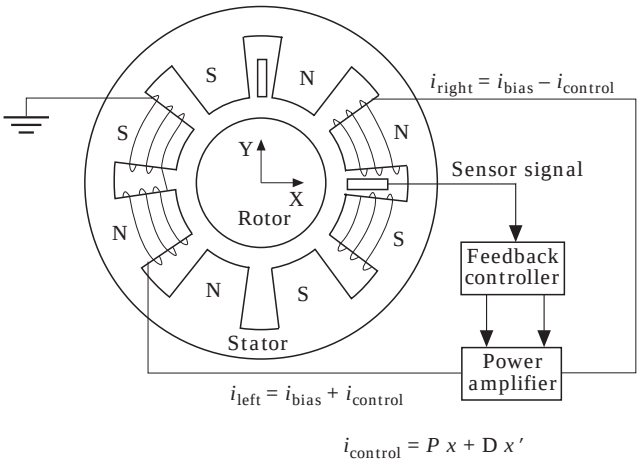

Figure 1. Rotor magnetic bearing system.

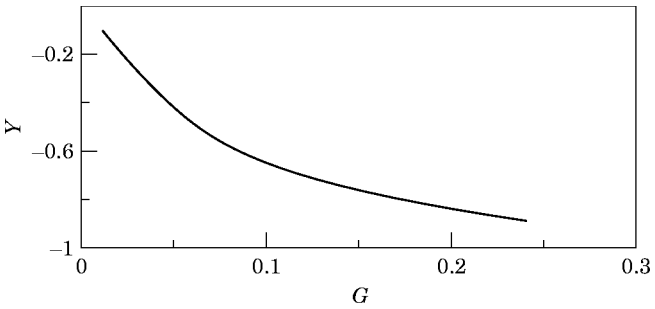

Figure 2. Locus of fixed points; $P = 1{\cdot}1$, $D = 0{\cdot}11$.

where the rotor co-ordinates x, y, and eccentricity, E, are non-dimensionalized with respect to bearing clearance; the time, τ, and rotor speed, Ω, are non-dimensionalized with respect to natural frequency; G is the dimensionless rotor weight term; α is the geometric coupling coefficient; and f's are the magnets' forces:

$$f_{r,l} = (1/(4P))\,[(1 \mp (Px + Dx'))/(1 \mp x)]^2, \qquad f_{t,b} = (1/(4P))\,[(1 \mp (Py + Dy'))/(1 \mp y)]^2, \tag{3, 4}$$

where P and D are the controllers' dimensionless proportional and derivative gains, respectively.

3. PERIODIC ORBITS

3.1. TRIGONOMETRIC COLLOCATION METHOD

In this method, a periodic solution is approximated by a Fourier series:

$$\{\mathbf{X}(\tau)\} = A_1 + \sum_{q=1}^{\mathscr{H}} [A_{2q} \cos(q\Omega_s \tau) + A_{2q+1} \sin(q\Omega_s \tau)], \tag{5}$$

where Ω_s is the smallest frequency of interest, $\mathscr{H}$ is the number of harmonics of Ω_s. For harmonic/superharmonic motion, $\Omega_s = \Omega$, and if a subharmonic with frequency a/b (a, b are integers) is sought, $\Omega_s = 1/b$. This series is substituted into the differential equations (1) and (2), and evaluated at $2\mathscr{H} + 1$ collocation nodes that are equally spaced over the fundamental period, $T(=2\pi/\Omega_s)$. This results in $2\mathscr{H} + 1$ non-linear algebraic equations in the $2\mathscr{H} + 1$ unknown A's. For bad initial guesses, more collocation nodes can be chosen

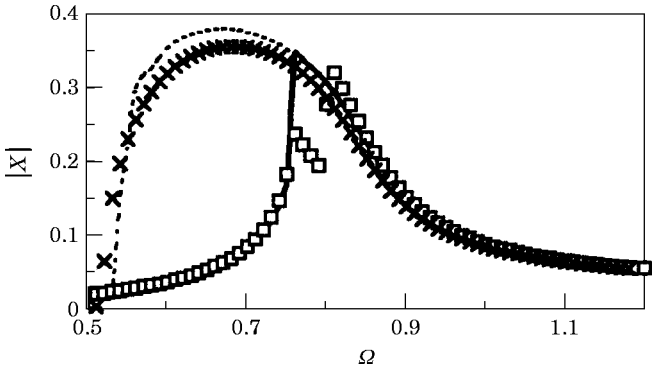

Figure 3. Non-linear frequency response; $P = 3$, $D = 0{\cdot}11$, $E = 0{\cdot}03$, $\alpha = G = 0$. Key: □, TCM increasing speed; ×, TCM decreasing speed; —, RK increasing speed; - - - -, RK decreasing speed.

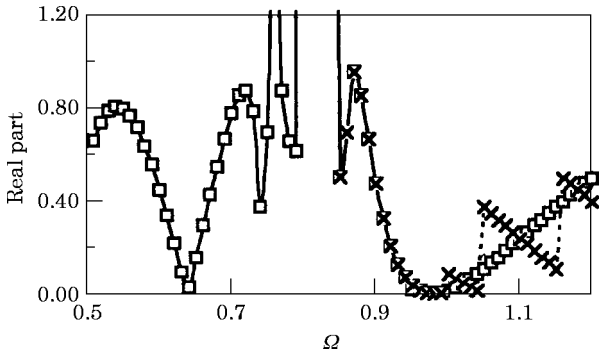

Figure 4. Floquet multiplier: real part, **X**-response; $P = 3$, $D = 0{\cdot}11$, $E = 0{\cdot}03$, $\alpha = G = 0$. Key: –□–, increasing speed; - - × - -, decreasing speed.

and a least squares algorithm used in solving the non-linear algebraic equations. Here, the Levenberg–Marquardt algorithm for non-linear least squares implemented in an IMSL [14] routine would be used.

3.2. FLOQUET THEORY: STABILITY AND BIFURCATION

The local stability of periodic motion of a non-linear system can be determined from Floquet theory. The theory can also predict the type of bifurcation of the periodic solution when a system parameter changes. In the following, the Floquet theory is given in brief and the stability and bifurcation conditions are noted.

To find the stability of a periodic solution $\{\mathbf{X}_0(\tau)\}$ of the system

$$\{\dot{\mathbf{X}}(\tau)\} = \{\mathbf{F}(\{\mathbf{X}\}, \tau)\}, \tag{6}$$

there should be at least one non-vanishing second derivative of $\{\mathbf{F}(\{\mathbf{X}\}, \tau)\}$ with respect to any element of $\{\mathbf{X}\}$. Let

$$\{\mathbf{X}(\tau)\} = \{\mathbf{X}_0(\tau)\} + \{\delta\mathbf{X}(\tau)\}. \tag{7}$$

Substituting equation (7) into equation (6), expanding $\{\mathbf{F}\}$ in a Taylor series about $\{\mathbf{X}_0\}$, and retaining only linear terms in the disturbance $\{\delta\mathbf{X}\}$ gives

$$\{\delta\dot{\mathbf{X}}(\tau)\} = [A(\tau)]\{\delta\mathbf{X}(\tau)\}, \tag{8}$$

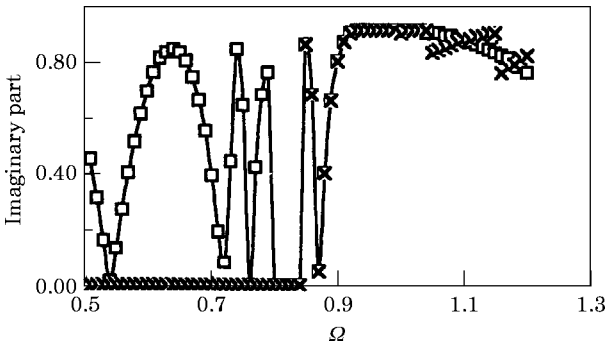

Figure 5. Floquet multiplier: imaginary part, **X**-response; $P = 3$, $D = 0{\cdot}11$, $E = 0{\cdot}03$, $\alpha = G = 0$. Key: –□–, increasing speed; - - × - -, decreasing speed.

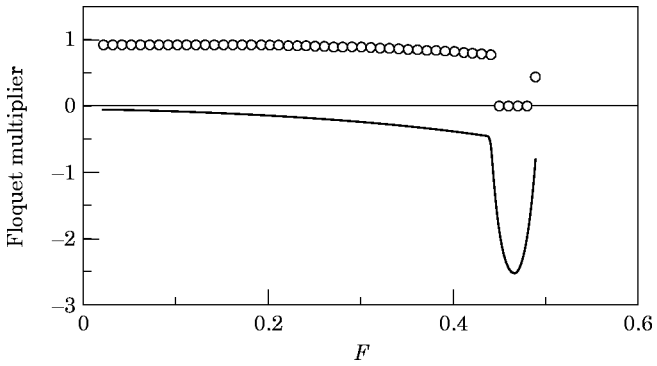

Figure 6. Period-doubling bifurcation; $P = 1{\cdot}1$, $D = 0{\cdot}03$, $G = 0{\cdot}03$, $\Omega = 1$, $\alpha = 0{\cdot}05$. —, real; ○, imaginary.

where $[\mathbf{A}(\tau)]$ is the matrix of first partial derivatives of $\{\mathbf{F}\}$ with respect to $\{\mathbf{X}\}$, and is periodic in time with period T. Equation (10) is a linear differential equation with periodic coefficients. For this magnetic bearing system, analytical expressions are obtained for the elements in matrix $[\mathbf{A}(\tau)]$. If the columns in

$$[\{\delta\mathbf{X}_1(0)\} \quad \{\delta\mathbf{X}_2(0)\} \cdots \{\delta\mathbf{X}_N(0)\}] = [I]_{N\times N} \tag{9}$$

are successively chosen as the initial conditions for equations (8), and $\{\delta\mathbf{X}(\tau)\}$ evaluated at T, then the monodromy matrix is

$$[\Phi] = [\{\delta\mathbf{X}_1(T)\} \quad \{\delta\mathbf{X}_2(T)\} \cdots \{\delta\mathbf{X}_N(T)\}]. \tag{10}$$

Its complex conjugate eigenvalues, δ_i, (Floquet multipliers) determine the local stability of the periodic solution. Here, equation (10) is solved using numerical integration for one period to obtain each column of $[\Phi]$, and in IMSL routine is used in solving for the eigenvalues. If $\delta_i < 1$, the solution is stable; $\delta_i > 1$, the solution is unstable; $\delta_i = 1$, stability cannot be determined from a linear analysis and non-linear terms have to be included.

When a unit circle in the complex plane is crossed by

a real eigenvalue on the positive real axis, it is a "cycle-fold" or "transcritical" bifurcation;

a pair of complex conjugate eigenvalues, it is a "secondary Hopf" bifurcation;

a real eigenvalue on the negative real axis, it is a "period-doubling" bifurcation. The "eigenvalue" discussed in this paragraph may be called the leading Floquet multiplier since

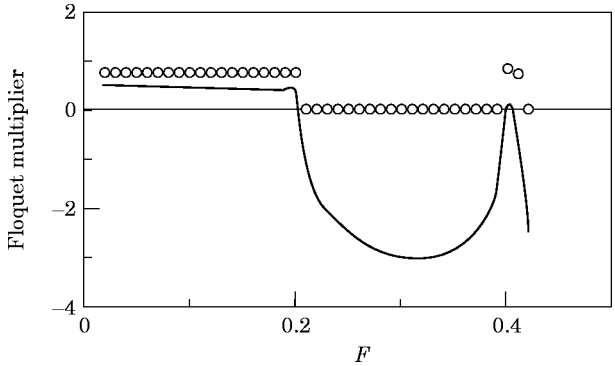

Figure 7. Period-doubling bifurcation; $P = 1{\cdot}1$, $D = 0{\cdot}03$, $G = 0{\cdot}03$, $\Omega = 1$, $\alpha = 0{\cdot}16$. Key as for Figure 6.

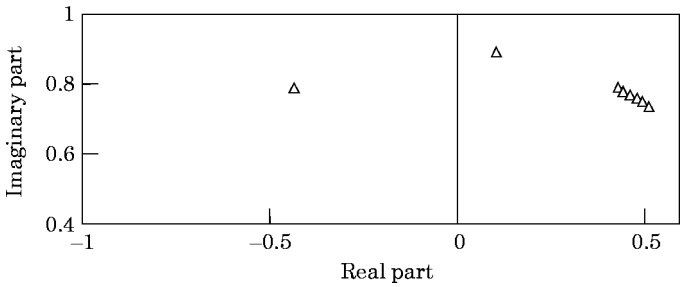

Figure 8. Floquet multiplier; $P = 1{\cdot}1$, $D = 0{\cdot}03$, $G = 0{\cdot}03$, $\Omega = 1$, $\alpha = 0{\cdot}16$.

it is the one which has the largest magnitude among all eigenvalues of the monodromy matrix.

In rotordynamics, cyclic-fold bifurcation is associated with the jump phenomenon, secondary-Hopf with quasiperiodic motion, and period-doubling with subsynchronous motion.

4. RESULTS AND DISCUSSION

To get an idea of the magnitude of the dimensionless weight parameter, G, the fixed points are obtained for a rotor–bearing system with no external forces ($E = F = 0$) and neglecting geometric coupling ($\alpha = 0$), using the trigonometric collocation method. (Note that these fixed points could just as well have been obtained by solving a non-linear algebraic equation in rotor position since velocity and acceleration terms are absent.) The bearing's feedback system has proportional gain, $P = 1{\cdot}1$ and derivative gain, $D = 0{\cdot}11$. Here, in the collocation method, only one collocation coefficient and collocation node each for x and y directions and zero initial guesses in each case are considered. The locus of the resulting fixed points is plotted in Figure 2. This method is much simpler than using numerical integration since in the latter method one has to filter many transient cycles depending on the damping before a stable fixed point is reached. This is more so if zero initial conditions are chosen. Furthermore, if zero initial conditions are chosen, numerical integration predicts a minimum possible $y = -0{\cdot}666$ ($G = 0{\cdot}1$) when in fact improving the initial condition for y gives the correct minimum $y = -0{\cdot}889$ ($G = 0{\cdot}24$). The trigonometric collocation method gave good results with zero initial guesses up to $G = 0{\cdot}23$ ($y = -0{\cdot}877$), but for the $G = 0{\cdot}24$ a better initial guess had to be chosen before the solution converged to the exact result. Here, the value of y corresponding to the previous value of $G(=0{\cdot}23)$ was chosen as the initial guess. Prior to changing the y initial guess,

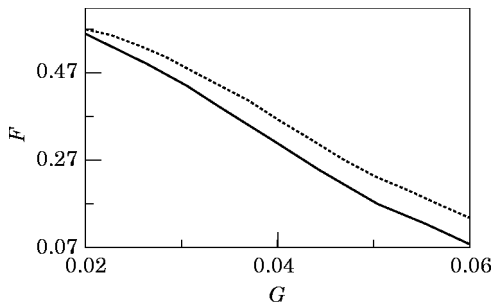

Figure 9. Stable period-1, period-2, and unstable regions; $P = 1{\cdot}1$, $D = 0{\cdot}03$, $\Omega = 1$, $\alpha = 0{\cdot}05$; —, P-1–P-2; - - - -, P-2–unstable.

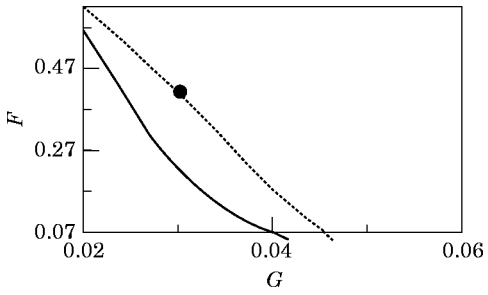

Figure 10. Stable period-1, period-2, and unstable regions; $P = 1{\cdot}1$, $D = 0{\cdot}03$, $\Omega = 1$, $\alpha = 0{\cdot}16$; —, P-1–P-2; - - - -, P-2–unstable; ●, P-4.

the number of collocation nodes was increased, but it had no effect in this case. For all the values of G shown, the leading Floquet multiplier is within the unit circle; hence the equilibrium positions are all stable.

Since rotor weight would be included in some of the simulations, the fixed point in the absence of harmonic force would not be (0, 0). The fixed point varies with rotor weight as given in Figure 2, and discussed in the preceding paragraph. Note that the fixed point could be brought up to (0, 0) by using more bias current for the top pole-pair than the bottom one and thus increasing the magnetic force in the positive y direction. While this is more common than having same bias currents, it is not included in the present model to avoid adding one more parameter into the system equations. Indeed having more bias current for the top pole-pair than the bottom one may change the rotor response characteristics, and needs to be investigated.

A frequency response curve can be obtained using the trigonometric collocation method. Here, the motion is assumed to have the same frequency as the rotor speed and only one harmonic. So, for x-motion, the collocation method would have only three coefficients: one, for the constant bias, and one each for cosine and sine terms. The minimum required collocation nodes (three) is chosen, and for simplicity all initial guesses for the coefficients are taken as zeros for the first value of speed. Subsequent initial guesses were the results from the previous value of speed. To verify the results obtained by this method, the response is also obtained by Runge–Kutta numerical integration of the equations of motion. Here also, for the first value of speed, the initial conditions were zeros, but for subsequent values of speed, the initial conditions were the results from the previous value of speed. The resulting frequency response curves obtained by both these methods, for both increasing and decreasing speed, are shown in Figure 3 for a softening bearing. The

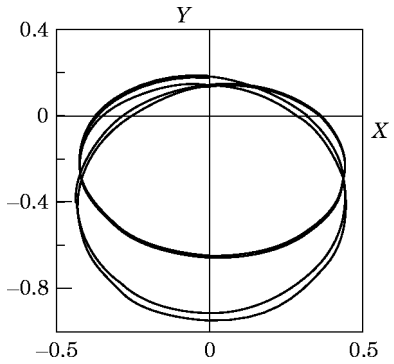

Figure 11. Period-4 orbit; $P = 1{\cdot}1$, $D = 0{\cdot}03$, $G = 0{\cdot}03$, $\Omega = 1$, $\alpha = 0{\cdot}16$.

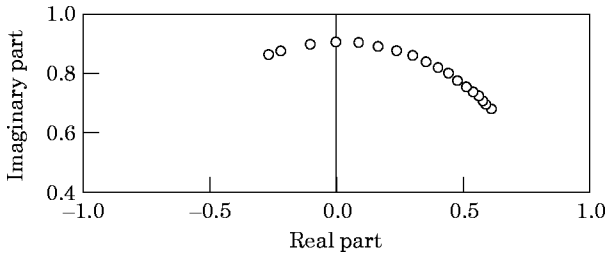

Figure 12. Floquet multiplier with collocation periodic solution; $P = 1{\cdot}1$, $D = 0{\cdot}03$, $G = 0{\cdot}03$, $\Omega = 1$, $\alpha = 0{\cdot}16$, $F = 0{\cdot}02$–2.

results from numerical integration are shown with lines, and those from collocation method with markers.

First, the results from numerical integration are discussed. For a non-linear imbalanced system, when the frequency is increased, the response increases continuously until it jumps to a peak amplitude and then the amplitude decreases continuously. Moreover, the response for decreasing frequency is not the same as the one for increasing frequency, and the region enclosed between jumps is the hysteresis region. For this system, as seen in Figure 3, the hysteresis region is rather small, implying a weak non-linearity. Even though the force from each pole-pair is strongly non-linear, the resulting force on the rotor in each co-ordinate direction is weakly non-linear because there is a pole-pair on either side of the rotor whose bias currents are the same and control currents are equal in magnitude but opposite in sign. The magnetic bearings are designed this way to reduce the non-linearity.

It may be noted from Figure 3 that the linearized natural frequency of the softening spring is approximately 0·82. This can also be obtained by linearizing the equation of motion, which gives a linearized natural frequency of $\sqrt{(P-1)/P}$. It can be shown that the magnetic bearing has hardening spring characteristics if $1 < P < 2$, and softening spring characteristics if $P > 2$. The frequency response characteristics of a hardening spring can be obtained similarly.

The results from the collocation method agree with those from numerical integration except in the hysteresis region. While numerical integration gives only stable solutions, the collocation method also gives unstable solutions. With the periodic solution obtained from the collocation method, the Floquet multipliers are computed, and the real and imaginary parts of the leading Floquet multipler are plotted in Figures 4 and 5. Note that Floquet's stability and bifurcation criteria are based directly on real and imaginary parts of the eigenvalues, and not directly on magnitude and phase, as discussed in section 3.2.

When the imaginary part of the Floquet multiplier is equal to zero and the real part becomes greater than one, then a cyclic-fold bifurcation that causes a "jump" results. This is seen in Figures 4 and 5. The results from the collocation method are stable and agree well with those obtained from numerical integration.

To study the effects of an external excitation force, F, whose amplitude is independent of the rotor speed, the equations of motion (1) and (2) are modified as

$$x'' = f_r - f_l + \alpha x(f_t + f_b) + F\cos\Omega\tau, \qquad y'' = f_t - f_b + \alpha y(f_r + f_l) + F\sin\Omega\tau - G. \tag{11, 12}$$

In investigating the effects of the excitation force, F, rotor weight, G, and geometric coupling, α, on the possible stable and unstable periodic regions, the other system parameters chosen are: proportional gain, $P = 1{\cdot}1$ (corresponds to a hardening spring). In simulations, a magnetic bearing with softening spring ($P > 2$) characteristics did not

show any period-doubling behavior. The other parameters chosen for the present analysis are derivative gain, $D = 0{\cdot}03$ (corresponds to 5% critical damping), and rotor speed, $\Omega = 1$, which is about three times the linearized natural frequency of 0·3. Two values of geometric coupling, α, are chosen here: 0·05 and 0·16. The $\alpha = 0{\cdot}05$ was the value obtained from modeling in reference [6], and $\alpha = 0{\cdot}16$ was the average experimental value reported in reference [13].

First, the effect of F would be studied for two values of α and one value of G. The non-linear equations of motion as well as the linear equations of motion with periodic coefficients resulting from Floquet theory are numerically integrated. For $G = 0{\cdot}03$, $\alpha = 0{\cdot}05$, Figure 6 shows how the real and imaginary parts of the leading Floquet multiplier varied with respect to the external force amplitude, F. For $F < 0{\cdot}45$, the eigenvalue is within the unit circle, so the motion is stable period-1. At $F = 0{\cdot}45$, the eigenvalue crossed the unit circle at -1 (imaginary part $= 0$); hence it is a "period-doubling" bifurcation, and the resulting motion is stable period-2. The period-2 region ends at $F = 0{\cdot}49$, when the rotor motion became unstable. If $\alpha = 0{\cdot}16$, the Floquet multiplier is shown in Figure 7, where the period-2 region is much wider. The Floquet multiplier in this case is also plotted as an Argand diagram in Figure 8, where F is implicit and the eigenvalue moved from right to left when F was increased.

The stability results presented are based on the x-direction response. The same stability characteristics but different amplitudes are obtained in the y direction; these are not included here. Rotor weight causes a negative offset for y motion, and geometric coupling is responsible for different x and y amplitudes. Note that bearing stiffness and damping are the same in the x and y directions.

Figures 6–8 presented results for only one value of $G(=0{\cdot}03)$. Now, the combined effect of F, G is studied for two values of α. For $\alpha = 0{\cdot}05$, the period-1, period-2, and unstable regions are plotted in an F–G diagram in Figure 9. Here, for values of F and G below the solid line the motion is period-1; between the lines the motion is period-2; above the broken line the motion is unstable. For $\alpha = 0{\cdot}16$, similar results are plotted in Figure 10. It is noted that at $G = 0{\cdot}02$ the rotor was stable for higher values of F for $\alpha = 0{\cdot}16$ when compared to that for $\alpha = 0{\cdot}05$. This is due to the rotor operating at a speed greater than the upper limit where jump occurs. A similar observation was made with regard to the effect of geometric coupling on a frequency response plot, disregarding G [6]. There is a period-4 motion for $\alpha = 0{\cdot}16$, $G = 0{\cdot}03$, $F = 0{\cdot}42$; the orbit is shown in Figure 11.

The Floquet multiplier shown in Figure 8 used the periodic solution obtained from numerical integration. When the periodic solution is obtained from collocation method, the Floquet multiplier is shown in Figure 12. Both show stable solutions for the same

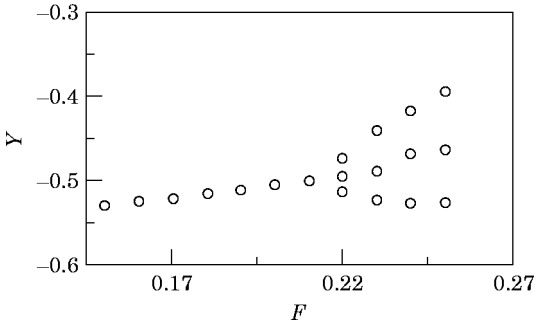

Figure 13. Period-doubling bifurcation: collocation method; $P = 1{\cdot}1$, $D = 0{\cdot}03$, $G = 0{\cdot}03$, $\Omega = 1$, $\alpha = 0{\cdot}16$.

parameter (F) range. In the collocation method, $\Omega_s = 1/2$, and for convergence, the number of harmonic terms $\mathscr{H} = 10$. This suggests that terms up to five times the running speed are important in the rotor response.

When a period-doubling bifurcation takes place, the stable period-1 motion before the bifurcation becomes an unstable period-1 motion after the bifurcation with the addition of a stable period-2 motion. The collocation method can be effectively used here to obtain both the unstable period-1 and stable period-2 motions after the bifurcation by choosing different initial guesses for the collocation coefficients. The resulting bifurcation diagram is shown in Figure 13, where the middle branch after bifurcation of the period-1 motion is unstable.

5. CONCLUSIONS

The collocation method is easy to use to find stable and unstable periodic orbits in a magnetic bearing. The orbits' stability and bifurcation behavior are readily predicted from Floquet theory. The motion of a rotor in a magnetic bearing undergoes cyclic-fold bifurcation resulting in jump when the frequency is varied. The rotor motion undergoes period-doubling bifurcation when the forcing amplitude is increased. The resulting subharmonic motion is present for a range of forcing amplitudes and rotor weights. The period-2 subharmonic range is small for small geometric coupling and is bigger for more geometric coupling. In the latter case, the motion was period-4 for one particular forcing amplitude.

REFERENCES

1. Y. Ishida 1994 *JSME International Journal*, Series C **37**, 237–245. Nonlinear vibrations and chaos in rotordynamics.
2. C. Nataraj 1995 *ASME/IGTI Congress*, Houston, Texas, **95-GT-204**. Nonlinear analysis of a rigid rotor on magnetic bearings.
3. A. M. Mohamed and F. P. Emad 1993 *IEEE Transactions on Automatic Control*, 1242–1245. Nonlinear oscillations in magnetic bearing systems.
4. K. V. Hebbale 1985 *Ph.D. Thesis*, *Cornell University*, A theoretical model for the study of nonlinear dynamics of magnetic bearings.
5. L. Virgin, T. F. Walsh and J. D. Knight 1995 *ASME Journal of Engineering for Gas Turbines and Power* **117**, 582–588. Nonlinear behavior of a magnetic bearing system.
6. M. Chinta, A. B. Palazzolo and A. Kascak 1996 Proceedings of Fifth International Symposium on Magnetic Bearings, Kanazawa, Japan, 147–152. Quasiperiodic Vibration of a rotor in a magnetic bearing with geometric coupling.
7. A. H. Nayfeh and Balachandran 1995 *Applied Nonlinear Dynamics*. New York: John Wiley.
8. R. H. B. Fey, D. H. van Campen and A. de Kraker 1992 *ASME Nonlinear Vibrations* **50**, 159–166. Long term structural dynamics of mechanical systems with local nonlinearities.
9. A. N. Jean and H. D. Nelson 1990 *Journal of Sound and Vibration* **143**, 473–489. Periodic response investigation of large order non-linear rotordynamic systems using collocation.
10. J. Y. Zhao, I. W. Linnett and L. J. McLean 1994 *ASME Journal of tribology* **116**, 361–368. Stability and bifurcation of unbalanced response of a squeeze film damped flexible rotor.
11. A. Buonomo 1992 *International Journal of Circuit Theory and Applications* **20**, 107–116. A collocation algorithm for calculating the periodic solutions of non-linear oscillators.
13. J. D. Knight, Z. Xia and E. B. McCaul 1992 *Proceedings of Third International Symposium on Magnetic Bearings*, Alexandria, Virginia, USA, 441–450. Forces in magnetic journal bearings: nonlinear computation and experimental measurement.
14. IMSL Fortran Library Version 3.0 1996 Visual Numerics, Inc., Houston, Texas.

APPENDIX: SYMBOLS

A	collocation coefficient
$[\mathbf{A}(\tau)]$	matrix of first partial derivatives of $\{\mathbf{F}\}$
D	derivative gain
E	mass eccentricity
F	external force amplitude
$\{\mathbf{F}\}$	force vector
f_r, f_l, f_t, f_b	forces of right, left, top, bottom magnets
G	rotor weight term
$\mathscr{H}$	number of harmonics in collocation method
P	proportional gain
T	period
$\{\mathbf{X}\}$	vector of state space variables
$\{\mathbf{X}_0\}$	periodic solution
x, y	rotor co-ordinates
α	geometric coupling coefficient
δ_i	Floquet multiplier
$\{\delta\mathbf{X}\}$	perturbation of periodic solution
τ	time
$[\mathbf{\Phi}]$	monodromy matrix
Ω	rotor speed
Ω_s	smallest frequency in collocation method